Nanoscale Research Letters
a SpringerOpen Journal

NANO EXPRESS Open Access

Improving scattering layer through mixture of nanoporous spheres and nanoparticles in ZnO-based dye-sensitized solar cells

Chohui Kim[1], Hongsik Choi[1], Jae Ik Kim[1], Sangheon Lee[1], Jinhyun Kim[1], Woojin Lee[1], Taehyun Hwang[1], Suji Kang[1], Taeho Moon[2*] and Byungwoo Park[1*]

Abstract

A scattering layer is utilized by mixing nanoporous spheres and nanoparticles in ZnO-based dye-sensitized solar cells. Hundred-nanometer-sized ZnO spheres consisting of approximately 35-nm-sized nanoparticles provide not only effective light scattering but also a large surface area. Furthermore, ZnO nanoparticles are added to the scattering layer to facilitate charge transport and increase the surface area as filling up large voids. The mixed scattering layer of nanoparticles and nanoporous spheres on top of the nanoparticle-based electrode (bilayer geometry) improves solar cell efficiency by enhancing both the short-circuit current (J_{sc}) and fill factor (FF), compared to the layer consisting of only nanoparticles or nanoporous spheres.

Keywords: Dye-sensitized solar cell; ZnO photoelectrode; Light trapping; Nanoparticle; Nanoporous sphere

Background

Dye-sensitized solar cells (DSSCs) have shown promising potential as an alternative to Si thin-film solar cells because of low fabrication cost and relatively high efficiency [1,2]. Efficient utilization of sunlight is greatly important in photovoltaic systems for high efficiency. Therefore, there have been many studies on the scattering layer to fully utilize incident light inside solar cells by using different morphologies and sizes of scatterers in TiO_2-based DSSCs [3-10]. However, few studies for the scattering layer exist in ZnO-based DSSCs [11-13], despite the advantages of ZnO such as higher carrier mobility and fabrication easiness for various nanostructures [14,15].

Among various nanostructures, hundred-nanometer-sized nanoporous spheres provide both effective light scattering and large surface area [16]. X. Tao's group and W. Que's group have reported on the scattering layer consisting of nanoporous spheres [17,18]. While they have shown improvements on the scattering effect, large voids between spheres leave the possibility of providing more available surface area where dye can be attached, and better charge transport by improved percolation of large-sized spheres should be achieved.

In this paper, we report the improvements of scattering layers using a mixture of nanoparticles and nanoporous spheres. Nanoporous spheres act as effective light scatterers with the large surface area, and nanoparticles favor both efficient charge transport and an additional surface area.

Methods

The ZnO nanoporous spheres were synthesized by using zinc acetate dihydrate (0.01 M, $Zn(CH_3COO)_2 \cdot 2H_2O$, Sigma-Aldrich, St. Louis, MO, USA) and diethylene glycol ($(HOCH_2CH_2)_2O$, Sigma-Aldrich) in an oil bath at 160°C for 6 h [16]. After washing with ethanol, the as-synthesized ZnO nanoporous spheres (NS) and ZnO nanoparticle (NP) (721085, Sigma-Aldrich) were mixed to the weight ratios of NP to NS of 10:0, 7:3, 5:5, 3:7, and 0:10. To fabricate bilayer-structured electrodes, a paste consisting of only ZnO nanoparticles (NP/NS = 10:0) was first spread on a fluorine-doped tin oxide substrate (FTO, TEC 8, Pilkington, St. Helens, UK) covered with a dense TiO_2 blocking layer by sputtering. After solvent evaporation, the

* Correspondence: taehom@dankook.ac.kr; byungwoo@snu.ac.kr
[2]Department of Materials Science and Engineering, Dankook University, Chungnam, Cheonan 330-714, South Korea
[1]WCU Hybrid Materials Program, Department of Materials Science and Engineering, Research Institute of Advanced Materials, Seoul National University, Seoul 151-744, South Korea

mixed pastes with various ratios of NS and NP were spread on top of the nanoparticle film by a doctor blade method. The active area was 0.28 cm^2, and the as-deposited films were subsequently annealed at 350°C for 1 h.

The films were sensitized with 0.5 mM of N719 dye ($RuL_2(NCS)_2$:2TBA, L = 2,2′-bipyridyl-4,4′-dicarboxylic acid, TBA = tetrabutylammonium, Solaronix, Aubonne, Switzerland) for 30 min at RT. The sensitized electrode and platinized counter electrode were sealed with thermoplastic foil (25 μm, DuPont, Wilmington, DE, USA), and the gap between the two electrodes was filled with an iodide-based redox electrolyte (AN-50, Solaronix).

X-ray diffraction (XRD; M18XHF-SRA, Mac Science, Tokyo, Japan) was employed to analyze the crystal structure of the ZnO electrodes, and field emission scanning electron microscopy (FE-SEM; SU70, Hitachi, Tokyo, Japan) was used to observe the morphology of the bilayer-structured electrodes. The electrochemical properties were analyzed by a solar cell measurement system (K3000, McScience, Suwon, South Korea) under a solar simulator (xenon lamp, air mass (AM) 1.5, 100 mW cm^{-2}). The extinction and diffused reflectance spectra were recorded on a UV/Vis spectrophotometer (Cary 5000, Agilent Technologies, Santa Clara, CA, USA), and incident photon-to-current conversion efficiency (IPCE) spectra were measured by an IPCE measurement system (K3100, McScience). Electrochemical impedance spectra (EIS) were taken by using a potentiostat (CHI 608C, CH Instrumental Inc., Austin, TX, USA) to analyze the kinetic parameters in the DSSCs [19-21].

Results and discussion

The crystalline structure and grain size of ZnO nanoparticles and nanoporous spheres were analyzed by XRD (Figure 1). The diffraction confirms the crystalline ZnO having hexagonal wurtzite structure (JCPDS #36-1451). From Williamson-Hall plots [22-24], the homemade ZnO nanoporous spheres are composed of approximately 35-nm-sized grains, while the grain size of the commercial ZnO nanoparticles is approximately 55 nm.

The ZnO bilayer electrodes were sequentially prepared by the bottom layer made by only ZnO nanoparticles and the top scattering layer formed with various mixing ratios of nanoparticles and nanoporous spheres. As shown in Figure 2, the plan-view SEM images of the scattering layers indicate that the nanoparticles and nanoporous spheres are mixed uniformly, not aggregated separately. The range of nanoporous sphere size is approximately 150 to 500 nm, with the average size of approximately 300 nm. As the ratio of nanoporous spheres increases, void spaces in the film get larger. The cross-sectional SEM images show that bilayer structures consisting of the nanoparticle bottom layer and mixed scattering upper layer are composed nicely without any

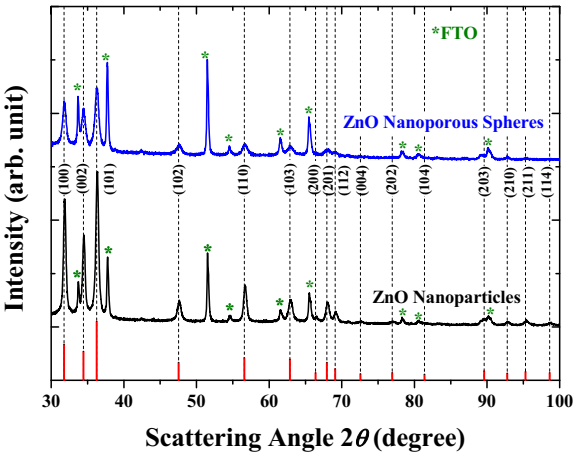

Figure 1 X-ray diffraction of the ZnO films consisting of only nanoparticles or nanoporous spheres. The peak intensities and positions from the hexagonal ZnO (JCPDS #36-1451) are shown as solid lines.

crushes at the interface The average thickness of the bilayer films is approximately 5.5 μm, and the deviation is less than 10%. The poor connectivity among the ZnO nanoporous spheres with the decreased nanoparticle ratio is consistent with the plan-view SEM images.

To investigate the optical properties of the mixed scattering layer, the diffused reflectance of the bilayer films (without dye) was measured (Figure 3a) [25,26]. With the increased nanoporous sphere ratio, the diffused reflectance increases, indicating a better light scattering ability of nanoporous spheres due to the comparable size to the wavelength of visible light [27,28]. The optical images also confirm the scattering effect by the nanoporous spheres. When the ratio reaches to NP/NS = 0:10, the color changes to totally white.

Furthermore, after dye adsorption, the NP/NS = 3:7 film shows the highest extinction (Figure 3b). Especially when compared to the NP/NS = 0:10 film, the higher extinction near the dye absorption peak is clear [29]. The results indicate an optimum condition for the surface area between void filling by nanoparticles and primary nanoporous spheres. The notable change in the curve shape for the NP/NS = 0:10 film (Figure 3a,b) means that light scattering plays a role considerably for the adsorbed dye molecules [30].

The solar cell performance of the DSSCs fabricated with the various ZnO bilayer electrodes was investigated (Figure 4a), and the parameters for each cell were summarized in Table 1 The mixed scattering layer improves both the short-circuit current (J_{sc}) and fill factor (FF), compared to the nanoparticle layer. In particular, the optimum power conversion efficiency (η) of 2.91% is obtained at the ratio of NP/NS = 3:7, and the trend of η is generally consistent with that of J_{sc}. The open-circuit

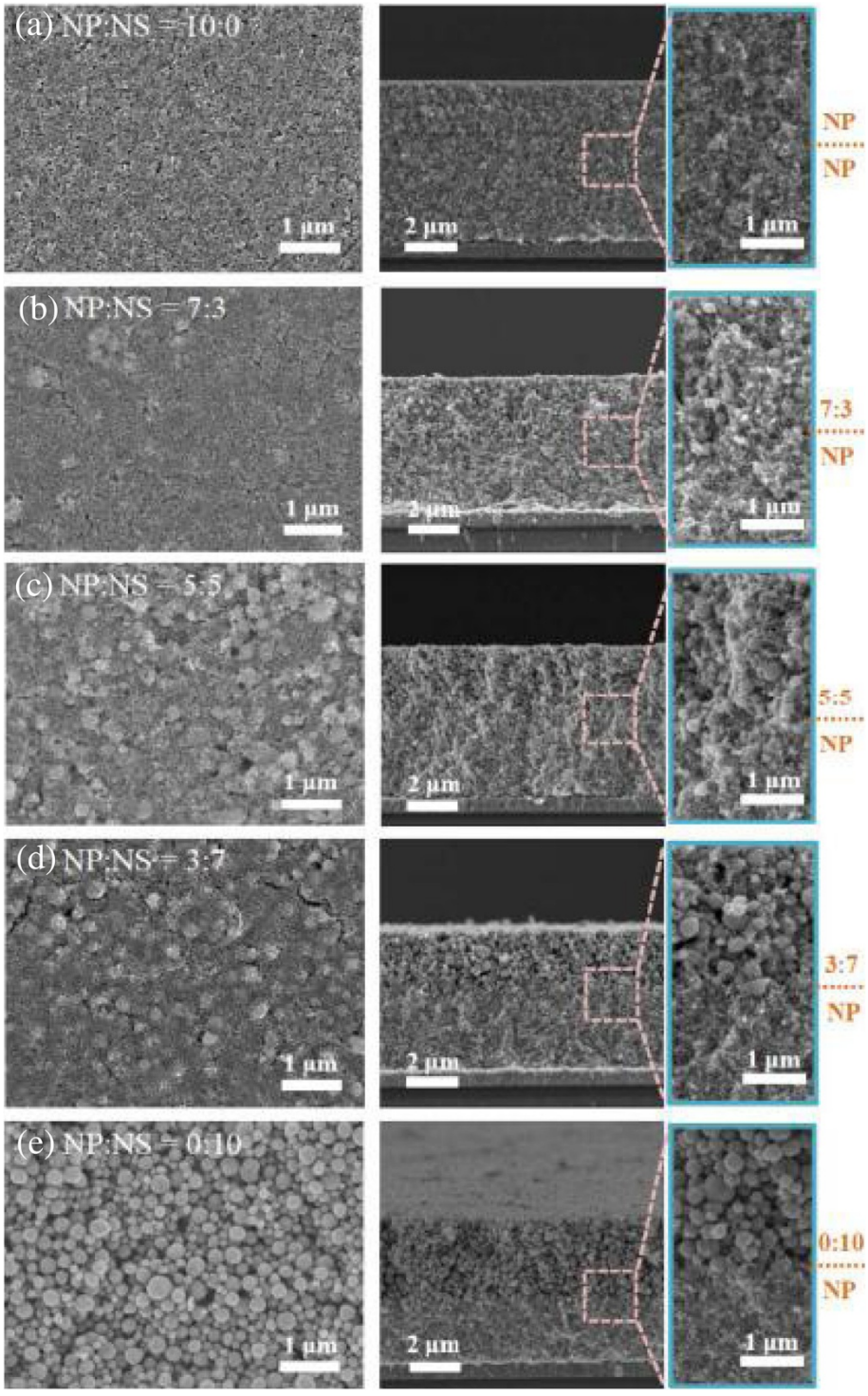

Figure 2 Plan-view and cross-sectional SEM images of the ZnO bilayer electrodes. The weight ratios of nanoparticle (NP) to nanoporous sphere (NS) for the top layers are **(a)** 10:0, **(b)** 7:3, **(c)** 5:5, **(d)** 3:7, and **(e)** 0:10, respectively. Blue labeled boxes are higher magnification for the bilayer interface.

voltage (V_{oc}) values are not notably changed among the cells except for the NP/NS = 3:7. From the general trend of parameters, we cautiously consider that the value for the open-circuit voltage in NP/NS = 3:7 is out of the tendency. We consider different nanomorphologies of porous spheres synthesized from the limited number of

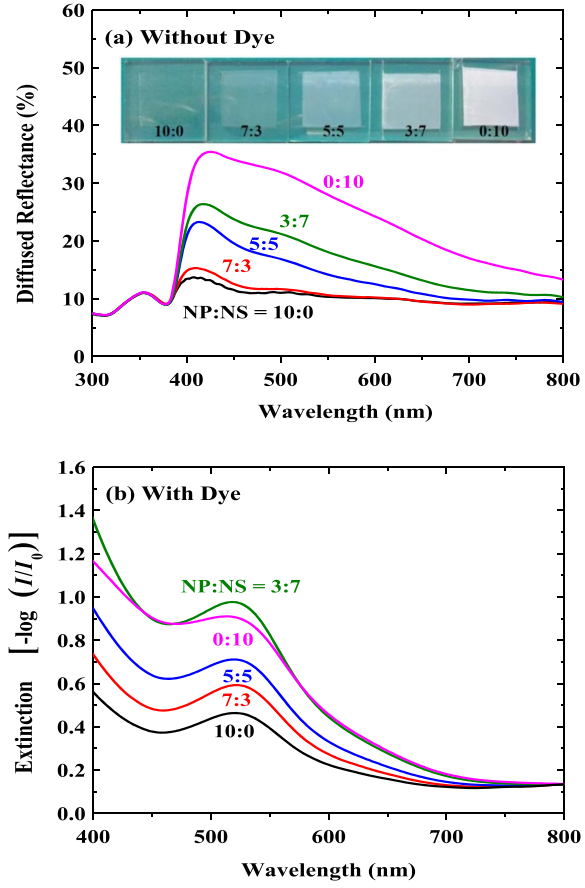

Figure 3 Diffused reflectance and extinction spectra. **(a)** Diffused reflectance spectra and optical images of the ZnO bilayer electrodes before dye loading with various mixing ratios. **(b)** Extinction spectra with dye loading.

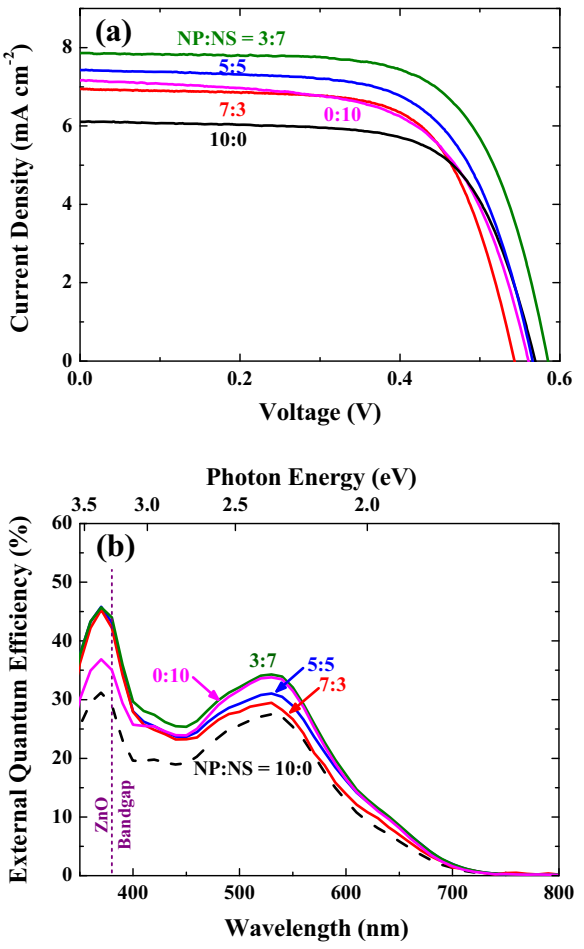

Figure 4 Photocurrent-voltage curves and IPCE spectra. **(a)** Photocurrent-voltage curves of the DSSCs with various mixing ratios. **(b)** Incident photon-to-current conversion efficiency (IPCE) spectra.

samples. Open-circuit voltage is represented as $V_{oc} \approx \frac{nkT}{q} \cdot \ln \frac{J_{sc}}{J_0}$ from the general one-diode model [31], and between the two conditions of the NP/NS = 5:5 and 3:7, the difference in J_{sc} (i.e., ln J_{sc}) is not enough to impact V_{oc}. Also, the change of V_{oc} may result from the difference of reverse saturation current J_0. We have synthesized nanoporous ZnO spheres by hydrothermal method [16], and the nanostructural quality of porous ZnO spheres may vary from batch to batch, thus resulting in the difference of band offset, charge transfer mobilities, porosities, etc. [32,33].

If charge collection probabilities are similar among the cells, quantum efficiency depends on the light trapping inside the solar cell [34-37]. The NP/NS = 3:7 cell exhibits the highest IPCE values in the whole visible region (Figure 4b), and this IPCE trend is consistent with the extinction data (Figure 3b). Therefore, the enhanced light-harvesting capability (i.e., J_{sc}) by the mixed scattering layer is attributed to efficient light scattering and increased surface area.

Impedance analyses were performed to understand the electrical properties of the synthesized solar cells [38-41]. The Nyquist plots display two semicircles in Figure 5a; the larger semicircles in low frequency range (approximately 10^0 to 10^3 Hz) are related to the charge transport/accumulation at dye-attached ZnO/electrolyte interfaces, and the smaller semicircles in high frequency (approximately 10^3 to 10^5 Hz) are ascribed to the charge transfer at the interfaces of electrolyte/Pt counter

Table 1 Characteristics of photocurrent-voltage curves and charge transfer resistances (R_{ct}) for ZnO/electrolyte interfaces

NP/NS	J_{sc} (mA cm^{-2})	V_{oc} (V)	FF	η (%)	R_{ct} (Ω)
10:0	5.98 ± 0.25	0.56 ± 0.01	0.67 ± 0.01	2.25 ± 0.15	30.7 ± 0.3
7:3	6.64 ± 0.30	0.55 ± 0.01	0.65 ± 0.02	2.36 ± 0.17	33.1 ± 0.2
5:5	7.45 ± 0.13	0.56 ± 0.01	0.68 ± 0.03	2.81 ± 0.14	29.8 ± 0.2
3:7	7.47 ± 0.24	0.58 ± 0.01	0.67 ± 0.01	2.91 ± 0.13	31.6 ± 0.2
0:10	7.28 ± 0.18	0.56 ± 0.01	0.64 ± 0.02	2.60 ± 0.09	34.5 ± 0.3

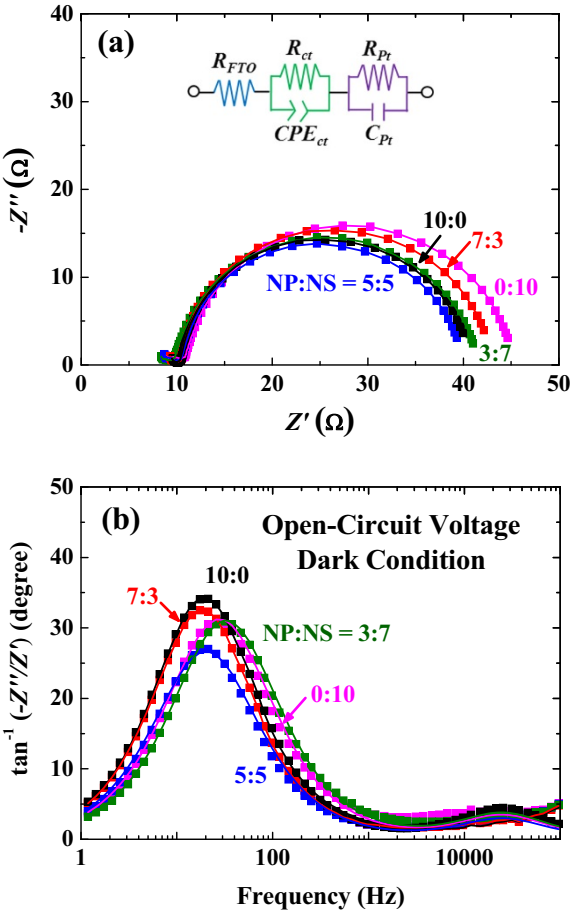

Figure 5 Plots with various mixing ratios of ZnO nanoparticle to nanoporous sphere. (a) Nyquist plot and **(b)** Bode plot. Solid lines are the fitting results using the equivalent circuit model in the inset.

electrode [42]. The impedance parameters were extracted using the equivalent circuit model (inset of Figure 5a), and the fitting lines are shown as solid lines in the Nyquist and Bode plots. From the charge transfer resistances (R_{ct}) in Table 1, we can see that the proper mixing ratio (e.g., 5:5 or 3:7) exhibits lower values implying more efficient charge transfer processes across the ZnO/electrolyte interfaces, while the pure nanoporous sphere layer (0:10) shows the highest R_{ct}. The low resistance favors the transport of the electrons injected within ZnO, thus eventually leading to an effective collection of electrons [11]. The better connectivity achieved by the nanoparticles likely facilitates charge transfer by providing electron transport pathways, thereby resulting in the enhancement of FF with less recombination.

Conclusions

To improve the utilization of scattering layer in ZnO-based DSSCs, nanoparticles and nanoporous spheres are mixed with various ratios. The nanoporous spheres play an important role in the scattering effect with the large surface area but possess disadvantages of large voids and point contacts between spheres. Nanoparticles clearly advance facile carrier transport with the additional surface area, thereby improving the solar cell efficiency by the enhanced short-circuit current (J_{sc}) and fill factor (FF).

Competing interests

The authors declare that they have no competing interests.

Authors' contributions

CK carried out the overall scientific experiment and drafted the manuscript. HC and JIK performed the FE-SEM measurements. SL carried out the analysis of electrochemical impedance spectra. JK and SK participated in the manuscript revision. WL and TH helped to check typing errors. BP and TM gave valuable advices about the whole experiments and manuscript as supervisors. All authors read and approved the final manuscript.

Acknowledgements

This research was supported by the National Research Foundation of Korea (NRF): 2013R1A1A2065793 and 2010–0029065.

Received: 4 March 2014 Accepted: 28 May 2014
Published: 11 June 2014

References

1. O'Regan B, Grätzel M: **A low-cost, high-efficiency solar cell based on dye-sensitized colloidal TiO_2 films.** *Nature* 1991, **353:**737–740.
2. Grätzel M: **Solar energy conversion by dye-sensitized photovoltaic cells.** *Inorg Chem* 2005, **44:**6841–6851.
3. Wang ZS, Kawauchi H, Kashima T, Arakawa H: **Significant influence of TiO_2 photoelectrode morphology on the energy conversion efficiency of N719 dye-sensitized solar cell.** *Coordin Chem Rev* 2004, **248:**13–14.
4. Chou CS, Guo MG, Liu KH, Chen YS: **Preparation of TiO_2 particles and their applications in the light scattering layer of a dye-sensitized solar cell.** *Appl Energ* 2012, **92:**224–233.
5. Sun X, Liu Y, Tai Q, Chen B, Peng T, Huang N, Xu S, Peng T, Zhao XZ: **High efficiency dye-sensitized solar cells based on a bi-layered photoanode made of TiO_2 nanocrystallites and microspheres with high thermal stability.** *J Phys Chem C* 2012, **116:**11859–11866.
6. Ke CR, Chen LC, Ting JM: **Photoanodes consisting of mesoporous anatase TiO_2 beads with various sizes for high-efficiency flexible dye-sensitized solar cells.** *J Phys Chem C* 2012, **116:**2600–2607.
7. Dadgostar S, Tajabadi F, Taghavinia N: **Mesoporous submicrometer TiO_2 hollow spheres as scatterers in dye-sensitized solar cells.** *ACS Appl Mater Interfaces* 2012, **4:**2964–2968.
8. Song J, Yang HB, Wang X, Khoo SY, Wong CC, Liu XW, Li CM: **Improved utilization of photogenerated charge using fluorine-doped TiO_2 hollow spheres scattering layer in dye-sensitized solar cells.** *ACS Appl Mater Interfaces* 2012, **4:**3712–3717.
9. Kang SH, Kim JY, Kim HS, Koh HD, Lee JS, Sung YE: **Influence of light scattering particles in the TiO_2 photoelectrode for solid-state dye-sensitized solar cell.** *J Photoch Photobio A* 2008, **200:**294–300.
10. Koo HJ, Park J, Yoo B, Yoo K, Kim K, Park NG: **Size-dependent scattering efficiency in dye-sensitized solar cell.** *Inorg Chem* 2008, **361:**677–683.
11. Zheng YZ, Tao X, Wang LX, Xu H, Hou Q, Zhou WL, Chen JF: **Novel ZnO-based film with double light-scattering layers as photoelectrodes for enhanced efficiency in dye-sensitized solar cells.** *Chem Mater* 2010, **22:**928–934.
12. He S, Zhang S, Lu J, Zhao Y, Ma J, Wei M, Evans DG, Duan X: **Enhancement of visible light photocatalysis by grafting ZnO nanoplatelets with exposed (0001) facets onto a hierarchical substrate.** *Chem Commun* 2011, **47:**10797–10799.
13. Zhang J, Que W, Jia Q, Zhong P, Liao Y, Ye X, Ding Y: **Novel bilayer structure ZnO based photoanode for enhancing conversion efficiency in dye-sensitized solar cells.** *J Alloy Compd* 2011, **509:**7421–7426.
14. Kaidashev EM, Lorenz M, Wenckstern H, Rahm A, Semmelhack HC, Han KH, Benndorf G, Bundesmann C, Hochmuth H, Grundmann M: **High electron**

mobility of epitaxial ZnO thin films on c-plane sapphire grown by multistep pulsed-laser deposition. *Appl Phys Lett* 2003, **82:**3901–3903.
15. Keis K, Vayssieres L, Rensmo H, Lindquist SE, Hagfeldt A: **Photoelectrochemical properties of nano- to microstructured ZnO electrodes.** *J Electrochem Soc* 2001, **148:**A149–A155.
16. Zhang Q, Chou TP, Russo B, Jenekhe SA, Cao G: **Aggregation of ZnO nanocrystallites for high conversion efficiency in dye-sensitized solar cells.** *Angew Chem Int Ed* 2008, **47:**2402–2406.
17. Park YC, Chang YJ, Kum BG, Kong EH, Son JY, Kwon YS, Park T, Jang HM: **Size-tunable mesoporous spherical TiO_2 as a scattering overlayer in high-performance dye-sensitized solar cells.** *J Mater Chem* 2011, **21:**9582–9586.
18. Yu IG, Kim YJ, Kim HJ, Lee C, Lee WI: **Size-dependent light-scattering effects of nanoporous TiO_2 spheres in dye-sensitized solar cells.** *J Mater Chem* 2011, **21:**532–538.
19. Nahm C, Choi H, Kim J, Byun S, Kang S, Hwang T, Park HH, Ko J, Park B: **A simple template-free 'sputtering deposition and selective etching' process for nanoporous thin films and its application to dye-sensitized solar cells.** *Nanotechnology* 2013, **24:**365604.
20. Kim J, Choi H, Nahm C, Moon J, Kim C, Nam S, Jung DR, Park B: **The effect of a blocking layer on the photovoltaic performance in CdS quantum-dot-sensitized solar cells.** *J Power Sources* 2011, **196:**10526–10531.
21. Choi H, Nahm C, Kim J, Moon J, Nam S, Kim C, Jung DR, Park B: **The effect of $TiCl_4$-treated TiO_2 compact layer on the performance of dye-sensitized solar cell.** *Curr Appl Phys* 2012, **12:**737.
22. Suryanarayana C, Norton MG: *X-ray Diffraction: A Practical Approach.* New York: Springer; 1998.
23. Kang J, Nam S, Oh Y, Choi H, Wi S, Lee B, Hwang T, Hong S, Park B: **Electronic effect in methanol dehydrogenation on Pt surfaces: potential control during methanol electrooxidation.** *J Phys Chem Lett* 2013, **4:**2931–2936.
24. Oh Y, Nam S, Wi S, Hong S, Park B: **Review paper: nanoscale interface control for high-performance Li-ion batteries.** *Electron Mater Lett* 2012, **8:**91–105.
25. Nahm C, Choi H, Kim J, Jung DR, Kim C, Moon J, Lee B, Park B: **The effects of 100 nm-diameter Au nanoparticles on dye-sensitized solar cells.** *Appl Phys Lett* 2011, **99:**253107.
26. Kim J, Choi H, Nahm C, Park B: **Review paper: surface plasmon resonance for photoluminescence and solar-cell applications.** *Electron Mater Lett* 2012, **8:**351–364.
27. Ferber J, Luther J: **Computer simulations of light scattering and absorption in dye-sensitized solar cells.** *Sol Energ Mat Sol C* 1998, **54:**265–275.
28. Ito S, Zakeerudiin SM, Humphry-Baker R, Liska P, Charvet P, Comte P, Nazeeruddin MK, Péchy P, Takata M, Miura H, Uchida S, Grätzel M: **High-efficiency organic-dye-sensitized solar cells controlled by nanocrystalline-TiO_2 electrode thickness.** *Adv Mater* 2006, **18:**1202–1205.
29. Ingle JDJ, Crouch SR: *Spectrochemical Analysis.* New Jersey: Prentice Hall; 1988.
30. Gálvez FE, Kemppainen E, Míguez H, Halme J: **Effect of diffuse light scattering designs on the efficiency of dye solar cells: an integral optical and electrical description.** *J Phys Chem C* 2012, **116:**11426–11433.
31. Lee JH, Cho S, Roy A, Jung HT, Heeger AJ: **Enhanced diode characteristics of organic solar cells using titanium suboxide electron transport layer.** *Appl Phys Lett* 2010, **96:**163303.
32. O'reagan BC, Durrant JR: **Kinetic and energetic paradigms for dye-sensitized solar cells: moving from the ideal to the real.** *Acc Chem Res* 2009, **42:**1799–1808.
33. Park DW, Jeong Y, Lee J, Lee J, Moon SH: **Interfacial charge-transfer loss in dye-sensitized solar cells.** *J Phys Chem C* 2013, **117:**2734–2739.
34. Kim C, Kim J, Choi H, Nahm C, Kang S, Lee S, Lee B, Park B: **The effect of TiO_2-coating layer on the performance in nanoporous ZnO-based dye-sensitized solar cells.** *J Power Sources* 2013, **232:**159–164.
35. Choi H, Kim J, Nahm C, Kim C, Nam S, Kang J, Lee B, Hwang T, Kang S, Choi DJ, Kim YH, Park B: **The role of ZnO-coating-layer thickness on the recombination in CdS quantum-dot-sensitized solar cells.** *Nano Energy* 2013, **2:**1218–1224.
36. Kim J, Choi H, Nahm C, Kim C, Kim JI, Lee W, Kang S, Lee B, Hwang T, Park HH, Park B: **Graded bandgap structure for PbS/CdS/ZnS quantum-dot-sensitized solar cells with a $Pb_xCd_{1-x}S$ interlayer.** *Appl Phys Lett* 2013, **102:**183901.
37. Chen Y, Huang F, Chen D, Cao L, Zhang XL, Caruso RA, Cheng YB: **Effect of mesoporous TiO_2 bead diameter in working electrodes on the efficiency of dye-sensitized solar cells.** *Chem Sus Chem* 2011, **4:**1498–1503.
38. Kim J, Choi H, Nahm C, Kim C, Nam S, Kang S, Jung DR, Kim JI, Kang J, Park B: **The role of a $TiCl_4$ treatment on the performance of CdS quantum-dot-sensitized solar cells.** *J Power Sources* 2012, **220:**108–113.
39. Choi H, Nahm C, Kim J, Kim C, Kang S, Hwang T, Park B: **Review paper: toward highly efficient quantu m-dot- and dye-sensitized solar cells.** *Curr Appl Phys* 2013, **13:**S2–S13.
40. Goes MS, Joanni E, Muniz EC, Savu R, Habeck TR, Bueno PR, Fabregat-Santiago F: **Impedance spectroscopy analysis of the effect of TiO_2 blocking layers on the efficiency of dye sensitized solar cells.** *J Phys Chem C* 2012, **116:**12415–12421.
41. Fabregat-Santiago F, Garcia-Belmonte JB, Boschloo G, Hagfeldt A: **Influence of electrolyte in transport and recombination in dye-sensitized solar cells studied by impedance spectroscopy.** *Sol Energ Mat Sol C* 2005, **87:**117–131.
42. Fabregat-Santiago F, Bisquert J, Palomares E, Otero L, Kuang D, Zakeeruddin SM, Grätzel M: **Correlation between photovoltaic performance and impedance spectroscopy of dye-sensitized solar cells based on ionic liquids.** *J Phys Chem C* 2007, **111:**6550–6560.

doi:10.1186/1556-276X-9-295
Cite this article as: Kim *et al.*: Improving scattering layer through mixture of nanoporous spheres and nanoparticles in ZnO-based dye-sensitized solar cells. *Nanoscale Research Letters* 2014 **9**:295.